Subtype specificity of scorpion β-toxin Tz1 interaction with voltage-gated sodium channels is determined by the pore loop of domain-3

Enrico Leipold, Alfred Hansel, Adolfo Borges, and Stefan H. Heinemann

Institute of Molecular Cell Biology, Research Unit "Molecular and Cellular Biophysics",

Medical Faculty of the Friedrich Schiller University Jena, Jena, Germany (E.L., A.H., S.H.H.);

and Sección de Biomembranas, Instituto de Medicina Experimental, Facultad de Medicina,

Universidad Central de Venezuela, Caracas, Venezuela (A.B.)

Running title: Subtype specificity of scorpion β-toxins

‡ Correspondence:

Prof. Dr. Stefan H. Heinemann

Institute of Molecular Cell Biology

Molecular and Cellular Biophysics

Friedrich Schiller University Jena

Drackendorfer Str. 1

D-07747 Jena, Germany

Tel: ++49-3641-9 32 56 80

Fax: ++49-3641-9 32 56 82

e-Mail: Stefan.H.Heinemann@uni-jena.de

Text pages: 20

Figures: 5

Tables: 1

References: 25

Abstract: 229 words

Introduction: 563 words

Discussion: 1339 words

Abbreviations:

Na_V channel, voltage-gated sodium channel.

Abstract

Voltage-gated sodium (Na$_V$) channels are modulated by a variety of specific neurotoxins.
Scorpion β-toxins affect the voltage-dependence of channel gating: In their presence Na$_V$
channels activate at sub-threshold membrane voltages. Previous mutagenesis studies have
revealed that the β-toxin Css4 interacts with the extracellular linker between segments 3 and
4 in domain-2 of Na$_V$ channels with the effect to trap this voltage sensor in an open position
(Cestèle et al., 1998, Neuron 21:919-931). The voltage sensor of domain-2 was thus
identified to constitute a major part of neurotoxin receptor site-4. Here we studied the effects
of the β-toxin Tz1 from the Venezuelan scorpion *Tityus zulianus* on various mammalian Na$_V$
channel types expressed in HEK 293 cells. While skeletal muscle channels (Na$_V$1.4) were
strongly affected by Tz1, the neuronal channels Na$_V$1.6 and Na$_V$1.2 were less sensitive, the
cardiac Na$_V$1.5 and the peripheral nerve channel Na$_V$1.7 basically insensitive. Analysis of
channel chimeras in which whole domains of Na$_V$1.2 were inserted into a Na$_V$1.4
background revealed that the Na$_V$1.2 phenotype was not conferred to Na$_V$1.4 by domain-2
but by domain-3. The interaction epitope could be narrowed down to residues E1251, K1252
and H1257 located in the C-terminal pore loop in domain-3. The receptor site for β-toxin
interaction with Na$_V$ channels is thus spanning domains 2 and 3 where the pore loop in
domain-3 specifies the pharmacological properties of individual neuronal Na$_V$ channel types.

Introduction

Voltage-gated sodium channels (Na$_V$ channels) consist of a large (~260 kDa) pore-forming α-subunit, composed of four homologous domains each with six transmembrane segments (S1-S6) and a hairpin-like pore region between S5 and S6, split in an N-terminal (SS1) and a C-terminal part (SS2). Na$_V$ channels play a pivotal role in cellular excitability and are targeted by a large variety of chemically distinct toxins (Janiszewski, 1990; Catterall, 1992; Gordon et al., 1998). Understanding the molecular mechanisms underlying the toxin action is not only important for toxicological research; various toxic substances serve as lead structures for novel therapeutics such as analgesics.

Scorpion venoms are a rich source of neurotoxins. Scorpion toxins affecting Na$_V$ channels typically are 60-76 residues long polypeptides comprising α- and β-toxins. They are classified according to their mode of action and binding properties to distinct sites (receptor sites-3 and -4, respectively) on Na$_V$ channels (Martin-Eauclaire and Couraud, 1995; Gordon et al., 1998; Possani et al., 1999; Zuo and Ji, 2004). While α-toxins inhibit rapid Na$_V$ channel inactivation, β-toxins show a rather complex effect. They shift the voltage dependence of channel activation to cause sub-threshold channel opening. Interestingly, this shift is enhanced when channels are preactivated by a depolarizing pulse. This led to the current picture of β-toxins being voltage-sensor toxins: They specifically interact with the voltage sensor in domain-2 of Na$_V$ channels to "trap" the sensor in an open position and, hence, to facilitate channel opening (Cestèle et al., 1998, 2001; Mantegazza and Cestèle, 2005).

These results have been obtained by elegant studies of Cestèle et al. (1998) who compared the effect of β-toxin Css4 (*Centruroides suffusus suffusus*) on rat brain sodium channels (Na$_V$1.2) with that on cardiac muscle sodium channels Na$_V$1.5. While Na$_V$1.2 was strongly affected by Css4, the toxin was without effect on the voltage dependence of Na$_V$1.5 activation. A mutagenesis approach revealed that a single residue (G845) located in the domain-2 S3-S4 linker of Na$_V$1.2 is critical for the toxin effect. When mutated to asparagine

as present in $Na_V1.5$ channels, the channel mutant was rendered insensitive to Css4. Interestingly, the identified glycine is conserved in most members of the mammalian Na_V channel gene family. It is found in central and peripheral nervous system channels ($Na_V1.1$-1.3, $Na_V1.6$, $Na_V1.7$) as well as in the skeletal muscle channels ($Na_V1.4$), anticipating that there may not be much subtype specificity for β-toxins in addition to the insensitivity of cardiac $Na_V1.5$. However, no systematic investigation of the effects of a single scorpion β-toxin on various types of mammalian Na_V channels under comparable conditions has been performed to date.

Therefore, we studied how Tz1, the major β-toxin from the Venezuelan scorpion *Tityus zulianus*, affects various mammalian Na_V channel types expressed in HEK 293 cells. As shown previously, Tz1 clearly shifts the voltage dependence of $Na_V1.4$ channel activation, but, similarly to Css4, has no effect on the activation of $Na_V1.5$ channels (Borges et al., 2004). Although the critical glycine residue is conserved in the neuronal channels $Na_V1.2$, $Na_V1.6$, and $Na_V1.7$ and in skeletal muscle channels ($Na_V1.4$), we find very diverse effects of Tz1 on these channel types. With channel chimera constructs we show that the subtype specificity is not determined by the voltage sensor of domain-2 but by the pore loop of domain-3. As a result, scorpion β-toxin receptor site-4 in Na_V channels consists of at least two major parts, one in domain-2 and one in domain-3.

Materials and Methods

Site-directed mutagenesis. The wild-type sodium channel constructs used in this study were the rat isoforms of $Na_V1.2$ (P04775; Noda et al., 1986) and $Na_V1.4$ (P15390; Trimmer et al., 1989), the human isoforms of $Na_V1.5$ (Q14524; Gellens et al., 1992) and $Na_V1.7$ (NP002968; Klugbauer et al., 1995), and the mouse isoform of $Na_V1.6$ (Q9WTU3; Kohrman et al., 1996). The construction of chimeras between $Na_V1.2$ and $Na_V1.4$ (2444, 4244, 4424, 4442, 44p(1.2)4, 22p(1.4)2) was described previously (Zorn et al., 2006). We used a similar approach to construct $Na_V1.4$ channels with the C-terminal part of the domain-3 pore loop from $Na_V1.5$, $Na_V1.6$ or $Na_V1.7$ (44p(1.5)4, 44p(1.6)4 or 44p(1.7)4), respectively. In $Na_V1.4$ we replaced nucleotides 3724-3864 by the homologous residues of $Na_V1.5$, $Na_V1.6$ or $Na_V1.7$. The amino acid substitutions in the resulting pore loop chimeras are as follows: 44p(1.2)4: E1251N, K1252V, E1254L, H1257K, V1260D; 44p(1.5)4: E1251G, K1252Y, H1257Q, Y1258W, V1260Y, L1266I; 44p(1.6)4: E1251K, K1252P, E1253D, H1257D, V1260D, L1262I, L1266I; 44p(1.7)4: R1250V, E1251N, K1252V, E1253D, E1254K, H1257K, V1260Y, N1261S, L1266I, I1270V (all $Na_V1.4$ numbering); 22p(1.4)2: N1436E, V1437K, L1439E, K1442H, D1445V ($Na_V1.2$ numbering). Single amino-acid substitutions Q657E, G658N, E1251N, K1252V, E1254L, H1257K and V1260D were introduced into $Na_V1.4$ using PCR-based site-directed mutagenesis. Primers were obtained from MWG (Ebersberg, Germany). All clones were verified by DNA sequencing. Plasmid DNA was isolated from *E. coli* using the Midi- or Maxi-plasmid purification kit (Qiagen, Hilden, Germany).

Cell culture and transfection. HEK 293 cells (CAMR, Porton Down, Salisbury, UK) were maintained in 45% Dulbecco's Minimal Eagles Medium (DMEM) and 45% F12, supplemented with 10% fetal calf serum in a 5% CO_2 incubator at 37°C. Cells were trypsinized, diluted with culture medium and grown in 35-mm dishes. When cells were grown to 30-50% confluence, transient transfection was performed using the Superfect transfection kit (Qiagen). HEK 293 cells were transfected with a 5:1 ratio of the Na_V channel expression plasmids and a vector encoding the CD8 antigen (Jurman et al., 1994). The cells were used

for electrophysiological recordings 2-3 days after transfection. Individual transfected cells were visualized with Dynabeads (Deutsche Dynal GmbH, Hamburg, Germany) binding to CD8.

Electrophysiological measurements. Whole-cell voltage clamp experiments were performed as described previously (Chen et al., 1999). Briefly, patch pipettes with resistances of 0.9-1.8 MΩ were used. The series resistance was compensated for by more than 80% in order to minimize voltage errors. A patch-clamp amplifier EPC10 was operated by PatchMaster software (both HEKA Elektronik, Lambrecht, Germany). Leak and capacitive currents were corrected with a p/n method. Currents were low-pass filtered at 5 kHz and sampled at a rate of 25 kHz. All experiments were performed at constant temperature, 19-21°C. Digitally filtered data (3 kHz) were analyzed using FitMaster (HEKA Elektronik) and IgorPro (WaveMetrics, Lake Oswego, OR, USA).

The patch pipettes contained (mM): 35 NaCl; 105 CsF; 10 EGTA; 10 Hepes (pH 7.4 with CsOH). The bath solution contained (mM): 150 NaCl; 2 KCl, 1.5 CaCl$_2$; 1 MgCl$_2$; 10 Hepes (pH 7.4 with NaOH). The application of toxin was performed with an application pipette as described previously (Chen et al., 1999).

To measure the use-dependence of Tz1 action, a double-pulse protocol was used (Borges et al. 2004). From a holding potential of –120 mV a set of test depolarizations in the range from –130 to +55 mV in steps of 5 mV was applied followed by a constant prepulse to –10 mV for 50 ms prior to a second set of test pulses with identical parameters as the first set. To ensure recovery from fast inactivation, the cells were held at –120 mV for 50 ms before and after the prepulse. The repetition interval was 5 s. Open probabilities (P_o) were calculated from current-voltage relationships:

$$I(V) = P_o(V)\, \Gamma_{max}\, V\, \frac{1 - e^{-(V - E_{rev})/25mV}}{1 - e^{-V/25mV}} \qquad \text{(eq. 1)}$$

Γ_{max} is the maximal conductance of all channels and E_{rev} the measured reversal potential. V is the test pulse voltage and I the peak test pulse current. For a quantitative data description

$$P_o(V) = \frac{1 - P_{tox}}{\left(1 + e^{-(V - V_m)/k_m}\right)^3} + \frac{P_{tox}}{\left(1 + e^{-(V - V_m - \Delta V)/k_m}\right)^2}$$ the open probabilities were plotted against the test pulse voltages and fit with a double Boltzmann formalism:

(eq. 2)

V_m is the half-maximal gate activation and k_m the corresponding slope factor. P_{tox} represents the probability of channels to be toxin-modified and ΔV is the voltage by which the activation of toxin-modified channels is shifted. In control experiments, i.e. in the absence of toxin, P_{tox} was set to 0. Using this formalism means to describe activation of control channels according to a Hodgkin & Huxley theory, i.e. using three independent activation gates. Toxin-modified channels are assumed to activate with two independent gates as one is trapped in an activated position. For a phenomenological description of channel opening the voltages for $P_o = 0.5$ ($V_{0.5}$) were back-calculated from eq. (2) and are provided in the figures and tables.

The voltage dependence of fast inactivation was assayed by conditioning cells for 500 ms at voltages ranging from −140 to −25 mV in steps of 5 mV and a repetition interval of 30 s. Subsequently, peak current was determined at −20 mV. The peak current plotted versus the conditioning voltage was described with a Boltzmann function. The holding potential was −120 mV in all cases.

All data were presented as mean ± standard error of the mean (n = number of independent experiments).

Toxin purification. **Tityus zulianus scorpions were collected near Santa Cruz de Mora, Mérida State, western Venezuela, and venom extracted by manual stimulation.** Tz1 was

purified from the crude venom using reverse phase HPLC essentially as described by Borges

et al. (2004).

Results

Effect of Tz1 on wild-type Na$_V$ channels. In a previous study we identified Tz1, the main

component in the venom of the Venezuelan scorpion *Tityus zulianus,* as a typical β-toxin that

shifts the half-maximal activation voltage of Na$_V$1.4 channels in the negative direction with an

apparent K_D of about 3.5 μM (Borges et al., 2004). Tz1, however, did not shift the activation

voltage of Na$_V$1.5 channels. Here we extended this study to neuronal sodium channels in

order to elucidate the subtype specificity of Tz1.

Na$_V$1.4, Na$_V$1.5 and the neuronal isoforms Na$_V$1.2, Na$_V$1.6, and Na$_V$1.7 were expressed in

HEK 293 cells and the voltage-dependent channel activation was investigated in the

absence and presence of 2 and 10 μM Tz1 using the whole-cell voltage-clamp technique.

Since a β-toxin-induced shift in the voltage dependence of activation can often be

potentiated by depolarizations preceding the test pulse, we applied a first series of test

voltages followed by a constant prepulse to preactivate the channels prior to a second test

pulse series. In Figure 1A current traces obtained at −70 mV, i.e. a voltage at which

channels are normally closed, are shown. This approach provides a measure of the Tz1

effect to lower the activation threshold of the channels with and without such a prepulse in

one experiment.

Figure 1B shows representative normalized conductance-voltage relationships of single cells

expressing Na$_V$1.4, Na$_V$1.6, Na$_V$1.2, Na$_V$1.7, and Na$_V$1.5 channels, respectively, under

control conditions and after application of 10 μM Tz1 in the absence and presence of a

prepulse. The vertical line marks −70 mV, a potential where channels are closed under

control conditions. P_{tox}, the probability of the channels to display a lowered activation

threshold is given in Table 1 and was derived from double Boltzmann fits of the normalized

conductance-voltage relationships (eq. 2). In Figure 1C P_{tox} is shown for the wild-type

channels with and without preactivation. Based on this analysis Na$_V$1.4 is the most sensitive

target for Tz1 with a P_{tox} value of about 67% followed by Na$_V$1.6 (23%) and Na$_V$1.2 (7%) for

10 µM Tz1. The shift of half-maximal channel activation, indicated by ΔV, was about –50 mV

for the neuronal isoforms $Na_V1.2$, $Na_V1.6$, and $Na_V1.7$. $Na_V1.4$ displayed a slightly less

pronounced activation shift of about –42 mV. Only a very small fraction of $Na_V1.5$ and $Na_V1.7$

channels was shifted by 10 µM Tz1 in the presence of a prepulse, the magnitude of ΔV,

however, was similar to that of the other channels. Tz1 therefore shifts activation of all

channel isoforms by about the same magnitude, but it exhibits pronounced subtype

specificity regarding the percentage of channels affected. It has a strong preference for the

skeletal muscle channel $Na_V1.4$ and differentiates well between neuronal sodium channels

in the order $Na_V1.6 >> Na_V1.2 > Na_V1.7$.

Analysis of the voltage sensor in domain-2. Cestèle et al. (1998) found that β-toxin Css4

strongly affects the activation of $Na_V1.2$ channels but does not modify the activation

threshold of $Na_V1.5$ channels. This difference could be attributed to a single site in the S3-S4

linker of domain-2: After mutating G845 in $Na_V1.2$ to asparagine (N), as present in $Na_V1.5$,

the channel became insensitive to Css4.

Similar to these results, Tz1 is unable to shift the activation threshold of $Na_V1.5$ suggesting

that the identified glycine residue could also be important for the action of Tz1. A direct

comparison of the amino acid sequences of the domain-2 S3-S4 linkers from $Na_V1.2$,

$Na_V1.4$, $Na_V1.5$, $Na_V1.6$, and $Na_V1.7$ reveals that G845 (numbering of $Na_V1.2$) is conserved

among the channels except for $Na_V1.5$ (Fig. 2A). Furthermore, compared to all channels

investigated, $Na_V1.5$ displays the least conserved domain-2 S3-S4 linker. Given that Tz1

discriminates between $Na_V1.4$, $Na_V1.6$, $Na_V1.2$, and $Na_V1.7$, the identified glycine cannot be

the sole molecular determinant for the subtype specificity of Tz1 shown in Figure 1.

Nevertheless, we first tested for the impact of the conserved glycine on the action of Tz1 by

constructing and assaying mutant G658N in the background of $Na_V1.4$. As shown in Figure

2B, the conductance-voltage relationship of $Na_V1.4$-G658N channels was not shifted by Tz1.

Thus, similarly to what Cestèle and coworkers (1998) found for Css4, the conserved glycine

in the domain-2 S3-S4 linker of Na_V channels is also crucial for the effect of Tz1 and is therefore of general importance.

However, as indicated by the alignment in Figure 2A, this position in the domain-2 S3-S4 linker cannot account for the differences found for the neuronal channels. To test whether or not this linker is important in this respect at all, we analyzed mutant Na_V1.4-E657Q as it represents an Na_V1.4 channel with the domain-2 S3-S4 linker of Na_V1.2. This mutant is as sensitive to Tz1 as the wild-type Na_V1.4 (Fig. 2B), i.e. it does *not* reflect properties of Na_V1.2. From this experiment we can safely conclude that the domain-2 S3-S4 linker is *not* the determinant for the subtype specificity of Tz1 with respect to neuronal Na_V channels.

Domain chimeras. Since there may be determinants outside the domain-2 S3-S4 linker responsible for the pronounced Tz1 subtype specificity, we applied a more rigorous approach by formation of domain chimeras between Na_V1.4 and Na_V1.2 channels, i.e. we inserted individual domains of Na_V1.2 into an Na_V1.4 background. The resulting four chimeric channels (domain-1: 2444; domain-2: 4244; domain-3: 4424; domain-4: 4442, see Fig. 3A) were expressed in HEK 293 cells and assayed for their response to 10 µM Tz1. Whereas 2444 and 4442 exhibited a phenotype very similar to Na_V1.4 channels, 4244 appeared more sensitive to Tz1 (Fig. 3, Table 1). Surprisingly, chimera 4424, a construct in which domain-3 was from Na_V1.2, showed a toxin sensitivity comparable to Na_V1.2 channels. As indicated in Table 1, all four domain chimeras displayed voltage-dependent gating parameters similar to that of wild-type Na_V1.4 channels. An altered gating behavior can therefore be excluded as the reason for their different sensitivities to Tz1. Thus, domain-3 seems to play a major role in determining the differential effects of Tz1 on neuronal Na_V channels.

Pore loop of domain-3. In order to further narrow down a putative interaction site, we analyzed a multiple sequence alignment of domain-3 from various Na_V channels and highlighted their pore domain as a region of high variability. In addition, previous binding studies of Cestèle et al. (1998) identified the C-terminal pore loop (SS2) of domain-3 as a

potential interaction site for the β-toxin Css4. An alignment (Fig. 4A) shows that $Na_V1.4$ and

$Na_V1.2$ only differ in five residues in this region. When the SS2 loop of domain-3 from $Na_V1.2$

was introduced into $Na_V1.4$, the resulting channel, 44p(1.2)4, became less sensitive to Tz1

(Fig. 4B, C, Table 1), comparable to $Na_V1.2$ wild-type channels. In order to rule out

nonspecific allosteric effects, we also constructed the reverse chimera 22p(1.4)2, i.e. a

construct in which the domain-3 SS2 loop of $Na_V1.4$ was inserted into $Na_V1.2$. This chimera

was readily sensitive to Tz1, comparable to wild-type $Na_V1.4$ channels. In addition, we

generated $Na_V1.4$ channel mutants with the domain-3 SS2 loops of $Na_V1.5$, $Na_V1.6$, and

$Na_V1.7$. As shown in Fig. 4 and Table 1, introduction of the SS2 loop from $Na_V1.5$ resulted in

channels with high sensitivity towards Tz1 (44p(1.5)4). Introduction of the SS2 loops from

$Na_V1.6$ and $Na_V1.7$ conferred the Tz1 sensitivity of the respective wild types (44p(1.6)4 and

44p(1.7)4, respectively). Thus, the SS2 loop of domain-3 critically determines how β-toxin

Tz1 interacts with voltage-gated sodium channels. The specific structures of the domain-3

SS2 loops from neuronal channels strongly diminish the action of Tz1, while the SS2 loop of

$Na_V1.5$ supports a Tz1 effect.

Single-site mutations in domain-3. Since the domain-3 SS2 loop completely conferred Tz1

sensitivity between the $Na_V1.2$ and $Na_V1.4$ wild-type channels, we analyzed the potential

structural determinants in more detail. As shown in Figure 4A, only five residues are different

between $Na_V1.2$ and $Na_V1.4$. Therefore, mutations yielding the residues of $Na_V1.2$ were

introduced into $Na_V1.4$. The analysis of these mutants, presented in Figure 5 and Table 1,

indicates that at least three amino-acid positions are crucial for Tz1-induced modulation of

the channel. The strongest effect of 10 µM Tz1 was measured in mutant H1257K reducing

P_{tox} to 17% followed by E1251N with a P_{tox} of 20% indicating their importance for the Tz1

subtype specificity. Interestingly, K1252V increased P_{tox} of $Na_V1.4$ from 67% to about 96%

making this mutant more sensitive to Tz1. Mutants E1254L and V1260D exhibited toxin

sensitivity slightly smaller than wild-type $Na_V1.4$ channels. Judging from the toxin effect at 2

and 10 μM, the sensitivity has the following order: K1252V > wild type > E1254L, V1260D >

E1251N, H1257K.

Like the replacement of whole channel domains, single-site substitutions in the domain-3

SS2 region had no noticeable influence on the gating properties of $Na_V1.4$ channels (Table

1). Therefore, the differential influence of the SS2 mutations on the Tz1 effect cannot be

accounted for alterations of channel gating. Instead, the results demonstrate that the SS2

region of domain-3 determines the subtype specificity of Na_V channels for the β-toxin Tz1.

Discussion

Subtype specificity of Tz1. Na_V channel-specific neurotoxins are intensively investigated gating modulators. According to their functional properties β-toxins can be clustered into (1) insect-selective toxins with an excitatory or depressant function, (2) classical mammalian-specific toxins, (3) toxins which are active on mammals and insects, and (4) toxins which compete with excitatory insect β-toxins as well as with classical α- and β-toxins for binding to the channels (Possani et al., 1999). Since recent research mostly concentrated on their specificity for different phyla (e.g. Shichor et al., 2002; Cohen et al., 2004; Bosmans et al., 2005), only little information is available about the specificity of β-toxins for different channel isoforms.

Using an electrophysiological approach we assayed for the first time the use-dependent potency of a scorpion β-toxin to alter the activation of the Na_V channel isoforms 1.2, 1.4, 1.5, 1.6, and 1.7. This functional approach revealed Tz1 as most active on the skeletal muscle channels Na_V1.4. The gating of about 67% of the Na_V1.4 channels expressed in transfected HEK 293 cells were modified by application of 10 µM Tz1, i.e. this fraction showed a half-maximal activation which was Tz1-shifted by more than –40 mV (Table 1). Qualitatively, the other channel types tested displayed a very similar shift in activation threshold. However, the percentage of channels affected by Tz1 was markedly reduced for Na_V1.2 and Na_V1.6 channels. The cardiac and peripheral nerve isoforms (Na_V1.5 and Na_V1.7, respectively) were basically insensitive to 10 µM Tz1. Thus, Tz1 strongly distinguishes between neuronal and muscular Na_V channels in a graded manner, giving rise to potential applications of β-toxins as research tools or even as pharmacologically relevant drugs.

Potential value of β-toxins. Since Na_V channel-specific scorpion toxins selectively modify either inactivation (α-toxins) or activation (β-toxins), they are proven tools for functional studies. Based on their Na_V channel-specific nature, Massensini et al. (2002) used fluorescently labeled members of both groups as probes for tracking Na_V channels in living

cells. Applications like these are important for studying complex neuronal networks. Assuming that the functional subtype specificity of Tz1 reflects subtype-specific binding to channels, this toxin could be used to track $Na_V1.4$ specifically. It should be feasible to develop specific probes on a toxin basis in order to uncover the Na_V channel composition in living material. Besides the potential as molecular probes for research, scorpion toxins are discussed to replace conventional insecticides because of resistances developed in some insect species against classically used agents like phyrethroids (Bosmans et al., 2005). The value of Tz1 for such purposes remains to be evaluated by analyzing its effect on insect sodium channels.

The strong specificity of some β-toxins also makes them ideal tools for studying Na_V channel defects. For example, a loss of $Na_V1.4$ function is the basis for hypokalaemic periodic paralysis of type 2 (hypoPP2; Sternberg et al., 2001), a skeletal muscle disorder. The pronounced $Na_V1.4$ specificity of Tz1 could be used to specifically "activate" hypoPP2 channels while promising to exhibit only limited neuronal and cardiac side effects when administered to experimental animals.

Identification of domain-3 as major interaction site. Gordon et al. (1992) showed that antibodies directed against the SS2 pore regions of domains 1, 3 and 4 of insect Na_V channels displaced radiolabeled $LqhIT_2$, an insect β-toxin from *Leiurus quinquestriatus hebraeus*, as well as AahIT, a β-toxin from *Androctonus australis hector*. In a further study Cestèle et al. (1998) constructed various chimeras between the differentially Css4-sensitive $Na_V1.2$ and $Na_V1.5$ channels in order to identify the sites that are important for binding this β-toxin. Although a glycine residue in the domain-2 S3-S4 linker of $Na_V1.2$ was identified as a major difference to $Na_V1.5$, the pore loops of domains 1 and 3 as well as the S1-S2 linker in domain-3 were found to have some impact on binding Css4.

Our strategy of analyzing the β-toxin – channel interaction was to start with the functional characterization of Tz1 on five different Na_V channel isoforms ($Na_V1.2$, $Na_V1.4$-1.7). This

approach revealed Tz1 as highly selective towards Na$_V$1.4 and able to distinguish with high potency between Na$_V$1.2, Na$_V$1.6, and Na$_V$1.7 channels. Using a step-by-step mutagenesis approach together with a functional assay, we identified the domain-3 SS2 pore region as the major molecular determinant for the β-toxin sensitivity of these channels: The domain-3 SS2 loops of the neuronal channels confer the Tz1 phenotypes to the respective wild-types to Na$_V$1.4 channels. This functional assignment does not hold for Na$_V$1.5: Although Na$_V$1.5 channels are insensitive towards Tz1, domain-3 SS2 from Na$_V$1.5 strongly enhances the Tz1 effect when inserted into a Na$_V$1.4 background. On the other hand, a Na$_V$1.5-like phenotype can be produced in Na$_V$1.4 channels by changing G658 to N as present in Na$_V$1.5 (Fig. 2), suggesting that a Na$_V$1.5-like domain-2 S3-S4 linker dominates a Na$_V$1.5-like domain-3 SS2 pore loop. These results indicate an exceptional role of Na$_V$1.5 with regard to scorpion β-toxins suggesting that the domain-3 SS2 loop of the Na$_V$1.5 channel is perfectly able to interact with Tz1, but the induction of a functional effect on channel gating is impaired by the specific structure of the domain-2 S3-S4 linker.

The observation that Na$_V$1.2 and Na$_V$1.4 only differ in five amino acid residues in the region pointed out as being important for the discrimination between the two channels by Tz1 prompted us to construct and assay single-site mutations for each of these residues. While the differences at positions 1260 and 1254 had a minor impact on toxin efficacy, an exchange of the histidine at position 1257 in Na$_V$1.4 to the lysine present in Na$_V$1.2 as well as the exchange of the negatively charged glutamate at position 1251 for asparagine present in Na$_V$1.2 both strongly impaired the toxin effect. Thus, the negative charge at position 1251 seems to support interaction with the toxin, possibly with a positively charged amino acid on the toxin as the counterpart. In the case of position 1257, the positive charge present in Na$_V$1.2 seems to impair interaction with the toxin as well. Intriguingly, a valine at the lysine-1252 position seems to support toxin interaction, since this mutant is even more sensitive for Tz1 than the most sensitive wild-type Na$_V$1.4 channel. In this case either the positive charge

or the bulkiness of the side chain may be decisive, since the neutral valine is also much smaller than lysine.

With these results on the impact of individual residues on the effect of Tz1 one may speculate about the expected sensitivity of other Na_V channels. The rat isoforms of $Na_V1.1$ and $Na_V1.3$ share a conserved domain-2 S3/S4 linker with $Na_V1.2$, differ, however, in the SS2 loop of domain-3. Since in $Na_V1.1$ the critical residues assayed in Fig. 5 are the same as in $Na_V1.2$, one can expect that $Na_V1.1$ is insensitive towards Tz1. The situation for $Na_V1.3$ is more complex: The SS2 loop in domain-3 differs in four residues from the sequence of $Na_V1.2$, among them are those residues that proved important for the Tz1 effect in our experiments. Since all residues mutated showed an impact on the Tz1 effect, the Tz1 sensitivity of $Na_V1.3$ cannot be predicted in a straightforward manner – it can be different to both, $Na_V1.2$ and $Na_V1.4$.

In conclusion, the scorpion β-toxin Tz1 is a valuable molecular tool as it discriminates well between various types of voltage-gated sodium channel isoforms, being most specific for channels from skeletal muscle. The subtype specificity for various neuronal channel types is not brought about, as initially assumed, by the classical receptor site-4, i.e., the domain-2 S3-S4 linker, but by the C-terminal pore loop (SS2) of domain-3. Therefore, receptor site-4 is composed of at least two major components, an interaction site determining the channel specificity in domain-3 and a site where the toxin interacts with the voltage sensor in domain-2. Based on recently obtained structural data of a voltage-gated potassium channel (Long et al., 2005), one can predict that the domain-2 S3-S4 linker and the domain-3 SS2 loop are very close in three-dimensional space such that a scorpion β-toxin with a diameter of about 3 nm could make contact to both functional modules of the sodium channel simultaneously.

Acknowledgments. We thank S. Arend for technical assistance.

References

Borges A, Alfonzo MJ, Garcia CC, Winand NJ, Leipold E, and Heinemann SH (2004) Isolation, molecular cloning and functional characterization of a novel β-toxin from the Venezuelan scorpion, *Tityus zulianus. Toxicon* **43:**671–684.

Bosmans F, Martin-Eauclaire MF, and Tytgat J (2005) The depressant scorpion neurotoxin LqqIT2 selectively modulates the insect voltage-gated sodium channel. *Toxicon* **45:**501–507.

Catterall WA (1992) Cellular and molecular biology of voltage-gated sodium channels. *Physiol Rev* **72:**15–48.

Cestèle S, Qu Y, Rogers JC, Rochat H, Scheuer T, and Catterall WA (1998) Voltage sensor-trapping: Enhanced activation of sodium channels by β-scorpion toxin bound to the S3-S4 loop in domain II. *Neuron* **21:**919–931.

Cestèle S, Scheuer T, Mantegazza M, Rochat H, and Catterall WA (2001) Neutralization of gating charges in domain II of the sodium channel α subunit enhances voltage-sensor trapping by a β-scorpion toxin. *J Gen Physiol* **118:**291–301.

Chen H, Gordon D, and Heinemann SH (1999) Modulation of cloned skeletal muscle sodium channels by the scorpion toxins Lqh II, Lqh III, and LqhαIT. *Pflügers Arch* **439:**423–432.

Cohen L, Karbat I, Gilles N, Froy O, Corzo G, Angelovici R, Gordon D, and Gurevitz M (2004) Dissection of the functional surface of an anti-insect excitatory toxin illuminates a putative "hot spot" common to all scorpion β-toxins affecting Na$^+$ channels. *J Biol Chem* **279:**8206–8211.

Gellens ME, George Jr AL, Chen LQ, Chahine M, Horn R, Barchi RL, and Kallen RG (1992) Primary structure and functional expression of the human cardiac tetrodotoxin-insensitive voltage-dependent sodium channel. *Proc Natl Acad Sci USA* **89:**554–558.

Gordon D, Moskowitz H, Eitan M, Warner C, Catterall WA, and Zlotkin E (1992) Localization of receptor sites for insect-selective toxins on sodium channels by site-directed antibodies. *Biochemistry* **31:**7622–7628.

Gordon D, Savarin P, Gurevitz M, and Zinn-Justin S (1998) Functional anatomy of scorpion toxins affecting sodium channels. *J Toxicol - Toxin Rev* **17:**131–159.

Janiszewski L (1990) The action of toxins on voltage-gated sodium channels. *Pol J Pharmacol Pharm* **42:**581–588.

Jurman ME, Boland LM, Liu Y, and Yellen G (1994) Visual identification of individual transfected cells for electrophysiology using antibody-coated beads. *Biotechniques* **17:**876–881.

Klugbauer N, Lacinova L, Flockerzi V, and Hofmann F (1995) Structure and functional expression of a new member of the tetrodotoxin-sensitive voltage-activated sodium channel family from human neuroendokrine cells. *EMBO J* **14:**1084−1090.

Kohrman DC, Smith MR, Goldin AL, Harris J, and Meisler MH (1996) A missense mutation in the sodium channel Scn8a is responsible for cerebellar ataxia in the mouse mutant jolting. *J Neurosci* **16:**5993–5999.

Long SB, Campbell EB, and MacKinnon R (2005) Crystal structure of a mammalian voltage-dependent Shaker family K$^+$ channel. *Science* **309**:897–903.

Mantegazza M and Cestèle S (2005) β-scorpion toxin effects suggest electrostatic interactions in domain II of voltage-dependent sodium channels. *J Physiol* **568:**13–30.

Martin-Eauclaire MF and Couraud F (1995) Scorpion neurotoxins: Effects and Mechanisms. In *Handbook of Neurotoxicology* (LW Chang & RS Dyer eds) pp 683–716, Marcel Dekker, NY.

Massensini AR, Suckling J, Brammer MJ, Moraes-Santos T, Gomez MV, and Romano-Silva
MA (2002) Tracking sodium channels in live cells: confocal imaging using fluorescently
labeled toxins. *J Neurosci Methods* **116:**189–196.

Noda M, Ikeda T, Suzuki H, Takeshima H, Takahashi T, Kuno M, and Numa S (1986)
Expression of functional sodium channels from cloned cDNA. *Nature* **322:**826–828.

Possani LD, Becerril B, Delepierre M, and Tytgat J (1999) Scorpion toxins specific for Na$^+$-
channels. *Eur J Biochem* **264:**287–300.

Shichor I, Zlotkin E, Ilan N, Chikashvili D, Stühmer W, Gordon D, and Lotan I (2002) Domain
2 of *Drosophila* para voltage-gated sodium channel confers insect properties to a rat brain
channel. *J Neuroscience* **22:**4364–4371.

Sternberg D, Maisonobe T, Jurkat-Rott K, Nicole S, Launay E, Chauveau D, Tabti N,
Lehmann-Horn F, and Hainque B (2001) Hypokalaemic periodic paralysis type 2 caused
by mutations at codon 672 in the muscle sodium channel gene SCN4A. *Brain* **124:**1091–
1099.

Trimmer JS, Cooperman SS, Tomiko SA, Zhou JY, Crean SM, Boyle MB, Kallen RG, Sheng
ZH, Barchi RL, Sigworth FJ, Goodman RH, Agnew WS, and Mandelet G (1989) Primary
structure and functional expression of a mammalian skeletal muscle sodium channel.
Neuron **3:**33–49.

Zorn S, Leipold E, Hansel A, Bulaj G, Olivera BM, Terlau H, and Heinemann SH (2006) The
μO-conotoxin MrVIA inhibits voltage-gated sodium channels by associating with domain-
3. *FEBS Letters* **580:**1360–1364.

Zuo XP and Ji YH (2004) Molecular mechanism of scorpion neurotoxins acting on sodium
channels. *Molecular Neurobiology* **30:**265–278.

Footnotes

Legends for Figures

Fig. 1. Effect of Tz1 on wild-type Na_V channels expressed in HEK 293 cells.

(**A**) Current responses of Na_V1.4, Na_V1.6, Na_V1.2, Na_V1.7, and Na_V1.5 channels to a test voltage of -70 mV, where channels are closed under control conditions (gray traces). Dashed traces represent currents in the presence of 10 µM Tz1 without a prepulse (–pp) and black traces with a prepulse (+pp). (**B**) Normalized conductance–voltage plots for the indicated channel types. Open circles: control conditions; open triangles: 10 µM Tz1 without preactivation; filled circles: 10 µM Tz1 with preactivation. (**C**) P_{tox} values for the indicated channels as horizontal histograms with (++pp) or without (–pp) a prepulse. The white bars indicate the P_{tox} values for 10 µM Tz1 (*n* see Table 1), the black bars for 2 µM Tz1 (*n* = 4 each).

Fig. 2. Analysis of the voltage sensor in domain-2.

(**A**) Alignment of the major part of receptor site-4, i.e. the S3-S4 linker of domain-2. (**B**) Normalized conductance–voltage plots for Na_V1.4 mutants G658N and E657Q and 10 µM Tz1 with a use of symbols as in Fig. 1. (**C**) P_{tox} values with a use of symbols as in Fig. 1. The triagles mark the P_{tox} values for wild-type Na_V1.2, the diamonds those for wild-type Na_V1.4 channels.

Fig. 3. Effect of 10 µM Tz1 on domain chimeras between Na_V1.4 and Na_V1.2.

(**A**) Cartoons illustrating the composition of the channel chimeras (Na_V1.4: white; Na_V1.2: black). (**B**) Normalized conductance–voltage plots for chimeras 2444, 4244, 4424, and 4442. (**C**) P_{tox} values. Symbols in B and C were used as in Figs 1 and 2.

Fig. 4. Pore loop chimeras.

(**A**) Alignment of the SS2 loop in domain-3 for Na$_V$1.4, Na$_V$1.2, Na$_V$1.6, Na$_V$1.7, and Na$_V$1.5.

(**B**) Normalized conductance–voltage plots for 44p(1.2)4, 22p(1.4)2, 44p(1.6)4, 44p(1.7)4, and 44p(1.5)4 before (open circles) and after application of 10 µM Tz1, with (filled circles) and without (open triangles) prepulse. (**C**) P_{tox} values. The dashed lines mark the P_{tox} values for the background channels (either Na$_V$1.2 or Na$_V$1.4), the solid lines those for the wild types that donated the domain-3 pore loop. Symbols in B and C were used as in Figs 1 and 2.

Fig. 5. Analysis of the domain-3 SS2 loop.

(**A**) Normalized conductance–voltage plots for mutants E1251N, K1252V, E1254L, H1257K, and V1260D in the background of Na$_V$1.4 before (open circles) and after application of 10 µM Tz1, with (filled circles) and without prepulse (open triangles). (**B**) P_{tox} values for 2 µM (black) and 10 µM Tz1 (white bars). The triagles mark the P_{tox} values for wild-type Na$_V$1.2, the diamonds those for wild-type Na$_V$1.4 channels. Symbols in A and B were used as in Figs 1 and 2.

Tables

Table 1. Parameters characterizing wild-type channels, channel chimeras, and single-site mutants

Channel	Activation			P_{tox}		n
	$V_{0.5}$ (mV)	ΔV (mV)	k_m (mV)	−pp (%)	+pp (%)	
Na$_V$1.4	-34.74 ± 2.51	-42.32 ± 0.94	8.65 ± 0.48	41.2 ± 2.9	66.8 ± 3.6	9
Na$_V$1.6	-35.15 ± 1.08	-49.29 ± 1.81	10.33 ± 0.51	8.4 ± 0.8	22.7 ± 2.5	7
Na$_V$1.2	-27.11 ± 3.23	-49.56 ± 0.75	10.38 ± 0.26	2.9 ± 0.9	7.1 ± 1.2	5
Na$_V$1.7	-34.72 ± 0.68	-49.52 ± 0.88	9.70 ± 0.84	0.5 ± 0.3	1.0 ± 0.3	4
Na$_V$1.5	-48.82 ± 2.93	-46.10 ± 0.43	11.14 ± 0.54	0.0 *	1.1 ± 0.4	4
2444	-35.56 ± 1.31	-41.31 ± 0.79	8.82 ± 0.22	38.6 ± 3.4	70.0 ± 3.8	4
4244	-32.56 ± 1.95	-39.67 ± 0.79	8.80 ± 0.17	70.8 ± 4.5	90.5 ± 2.4	5
4424	-32.49 ± 2.41	-39.25 ± 1.45	7.62 ± 0.76	7.6 ± 1.3	10.9 ± 1.7	5
4442	-38.77 ± 2.76	-42.17 ± 0.51	8.78 ± 0.45	35.4 ± 3.2	59.4 ± 4.4	6
44p(1.2)4	-36.25 ± 1.85	-41.54 ± 1.97	7.71 ± 0.35	4.5 ± 0.5	7.9 ± 0.9	5
44p(1.5)4	-40.27 ± 2.92	-40.62 ± 0.81	7.74 ± 0.28	76.6 ± 2.6	96.9 ± 1.7	4
44p(1.6)4	-38.05 ± 2.71	-44.44 ± 1.17	8.18 ± 0.21	22.6 ± 1.9	37.5 ± 3.2	6
44p(1.7)4	-31.45 ± 1.79	-45.21 ± 0.42	9.47 ± 0.68	0.3 ± 0.3	1.5 ± 0.5	5
22p(1.4)2	-31.86 ± 1.62	-39.47 ± 0.48	10.59 ± 0.43	55.0 ± 3.1	87.5 ± 0.6	4
Q657E	-39.71 ± 1.46	-38.54 ± 1.07	7.78 ± 0.45	41.5 ± 5.7	58.3 ± 7.1	6
G658N	-39.60 ± 2.38	-46.68 ± 3.27	10.93 ± 1.51	2.6 ± 1.2	3.7 ± 1.5	5
E1251N	-37.52 ± 3.31	-41.81 ± 0.89	7.83 ± 0.67	8.8 ± 1.0	20.2 ± 2.7	5
K1252V	-34.82 ± 1.44	-39.28 ± 0.49	8.14 ± 0.32	68.0 ± 2.3	95.3 ± 0.7	4
E1254L	-34.99 ± 1.27	-41.04 ± 0.57	8.47 ± 0.24	50.0 ± 2.3	57.2 ± 2.9	5

| H1257K | -34.85 ± 2.63 | -39.84 ± 0.83 | 7.77 ± 0.57 | 6.8 ± 1.0 | 16.7 ± 2.1 | 5 |
| V1260D | -31.54 ± 2.76 | -39.13 ± 1.31 | 8.58 ± 0.88 | 40.1 ± 3.0 | 61.7 ± 4.2 | 5 |

Current-voltage relationships of the indicated channel isoforms and mutants before and after application of 10 μM Tz1 were analyzed according to eqn 1 and 2 to yield the voltage where 50% of the channels are opened under control conditions ($V_{0.5}$) and the corresponding slope factor for a single gate (k_m). Application of Tz1 shifted channel activation by ΔV. The P_{tox} values indicate the percentage of channels being Tz1-modified in the absence (–pp) and presence (+pp) of a conditioning prepulse. n is the number of independent experiments. * no measurable effect.
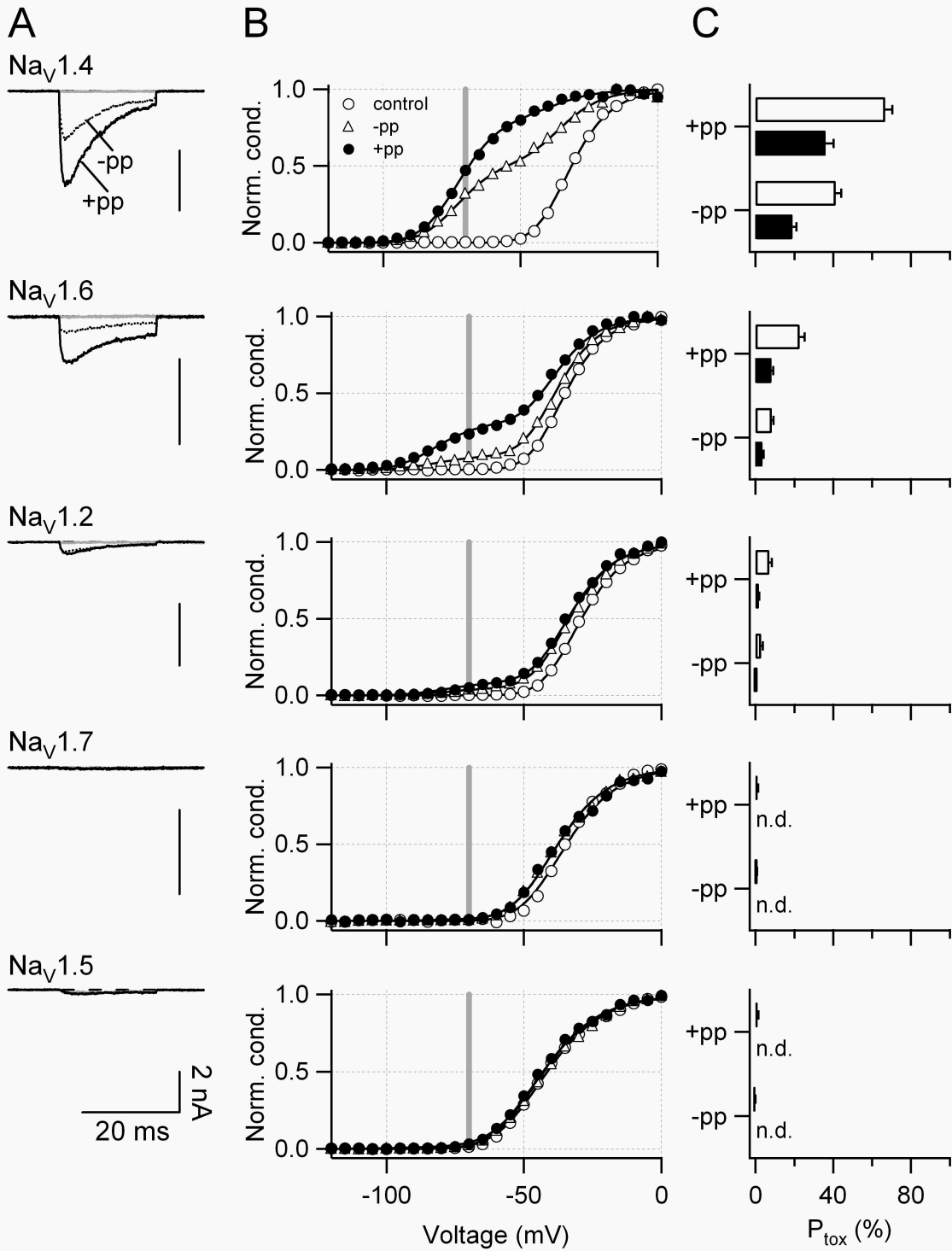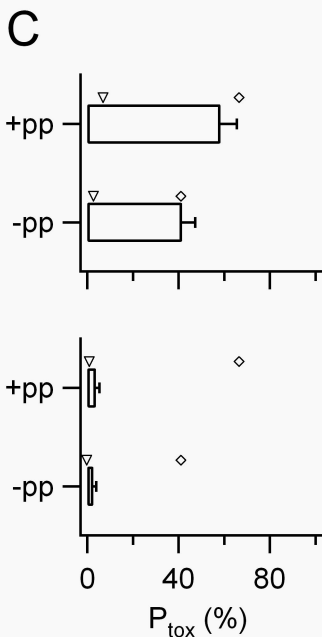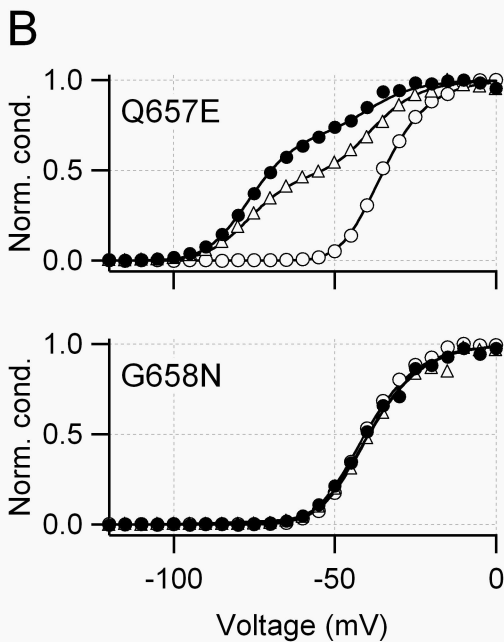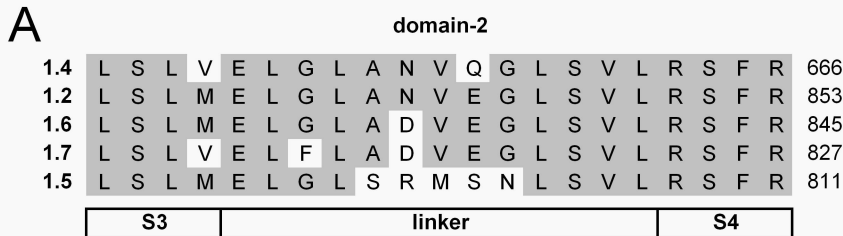
A

Na$_V$1.4

-pp
+pp

Na$_V$1.6

Na$_V$1.2

Na$_V$1.7

Na$_V$1.5

2 nA

20 ms

B

○ control
△ -pp
● +pp

Norm. cond.

1.0

0.5

0.0

Voltage (mV)

-100   -50   0

C

+pp

-pp

+pp

n.d.

-pp

n.d.

+pp

n.d.

-pp

n.d.

P$_{tox}$ (%)

0   40   80

Figure 1

domain-2

1.4	L	S	L	V	E	L	G	L	A	N	V	Q	G	L	S	V	L	R	S	F	R	666
1.2	L	S	L	M	E	L	G	L	A	N	V	E	G	L	S	V	L	R	S	F	R	853
1.6	L	S	L	M	E	L	G	L	A	D	V	E	G	L	S	V	L	R	S	F	R	845
1.7	L	S	L	V	E	L	F	L	A	D	V	E	G	L	S	V	L	R	S	F	R	827
1.5	L	S	L	M	E	L	G	L	S	R	M	S	N	L	S	V	L	R	S	F	R	811

S3 — linker — S4
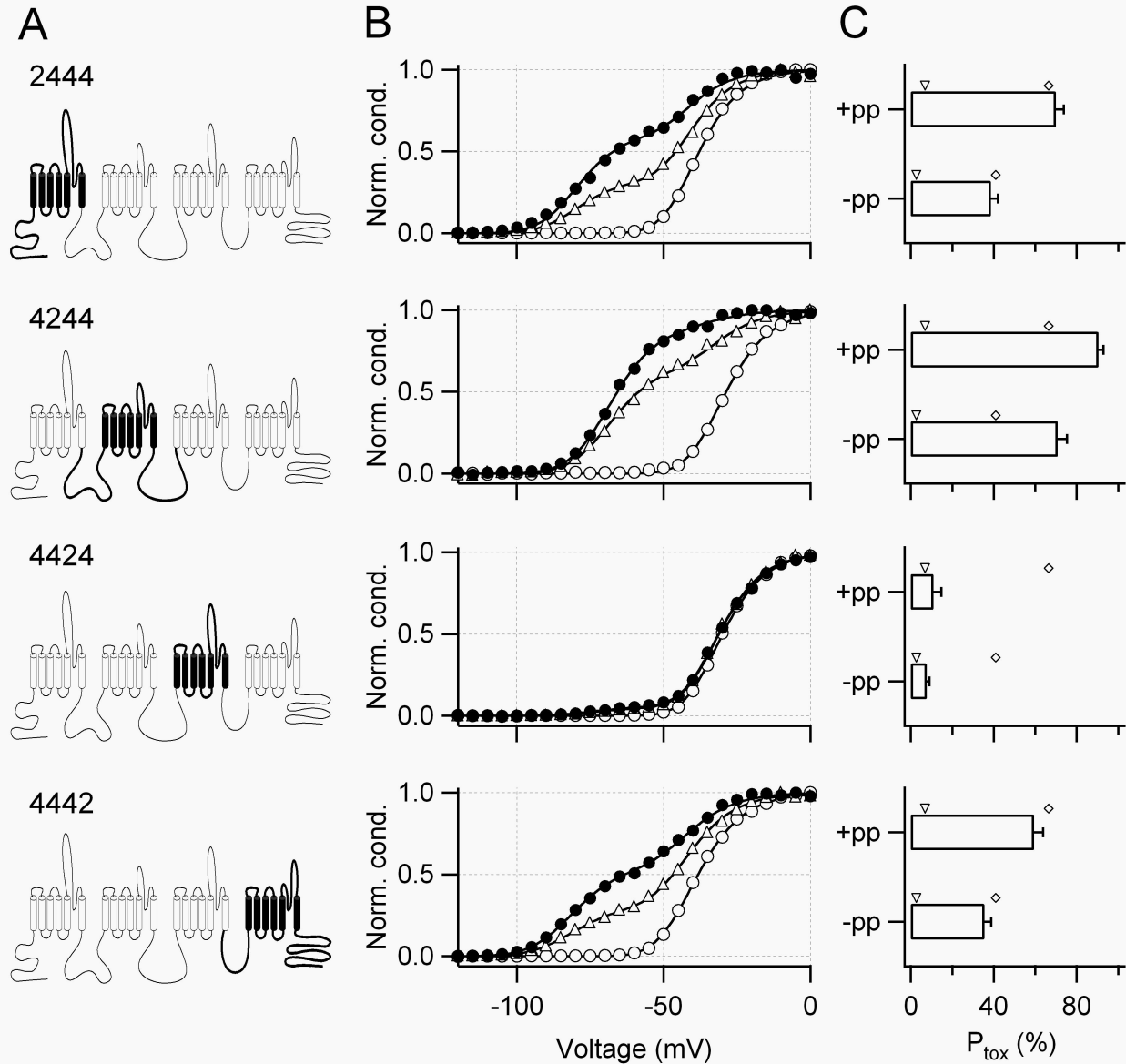
Figure 2

Figure 3

A

domain-3

1.4	A	A	V	D	S	R	E	K	E	E	Q	P	H	Y	E	V	N	L	Y	M	Y	1265
1.2	A	A	V	D	S	R	N	V	E	L	Q	P	K	Y	E	D	N	L	Y	M	Y	1450
1.6	A	A	V	D	S	R	K	P	D	E	Q	P	D	Y	E	G	N	I	Y	M	Y	1439
1.7	A	A	V	D	S	V	N	V	D	K	Q	P	K	Y	E	Y	S	L	Y	M	Y	1423
1.5	A	A	V	D	S	R	G	Y	E	E	Q	P	Q	W	E	Y	N	L	Y	M	Y	1447

SS2 pore loop — S6

B 44p(1.2)4, 22p(1.4)2, 44p(1.6)4, 44p(1.7)4, 44p(1.5)4

Norm. cond. vs Voltage (mV)

C P_{tox} (%)

Figure 4

Figure 5